Supplementary Figure 1

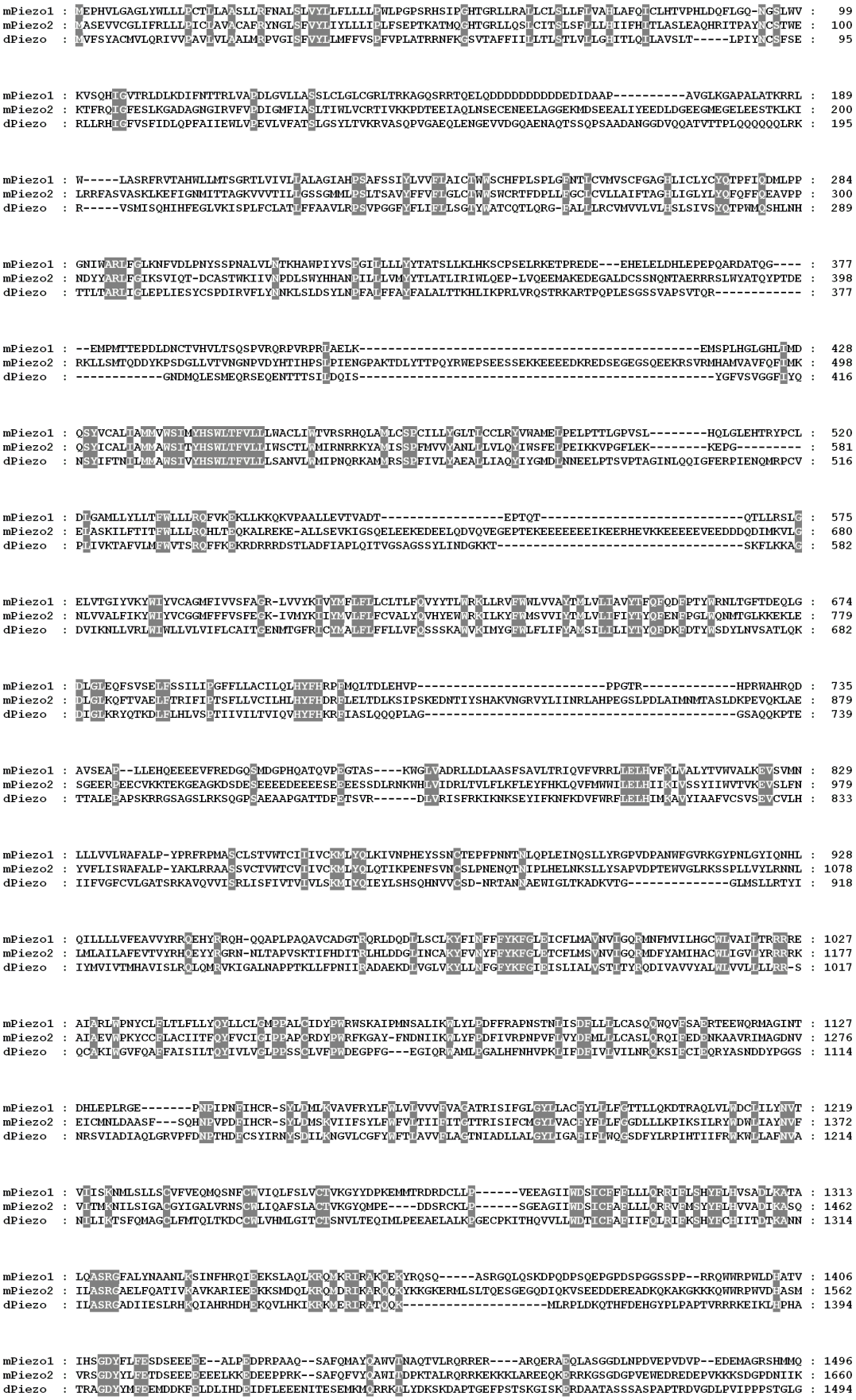

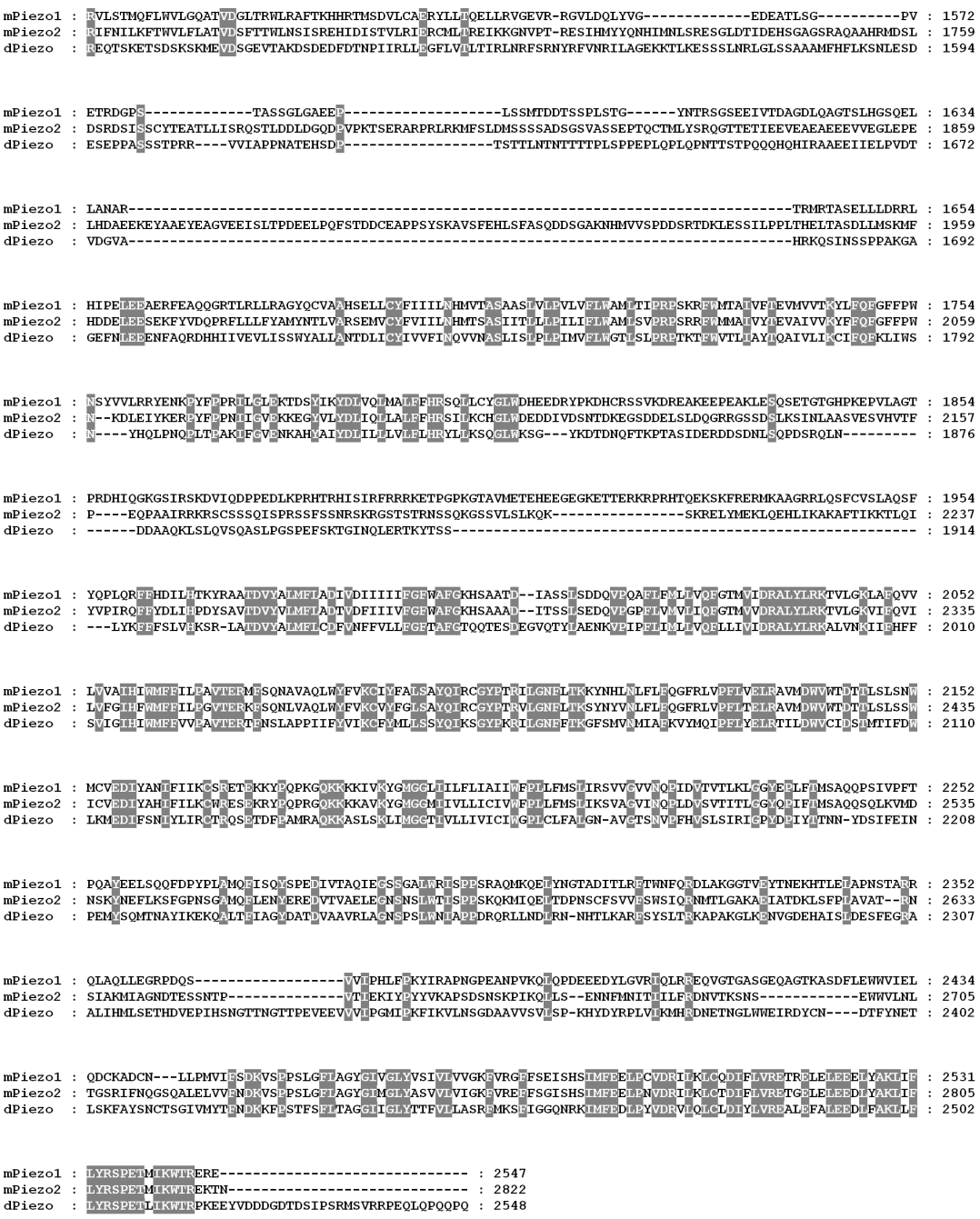

Supplementary Figure 1. Conservation between mouse and drosophila Piezos.

Alignment of mpiezo1, mpiezo2 and dpiezo proteins. Conserved identical residues are highlighted in gray. dpiezo is 24% identical to both mpiezo1 and mpiezo2. Alignment was done with ClustalW and further analyzed using Genedoc program.

Supplementary Figure 2

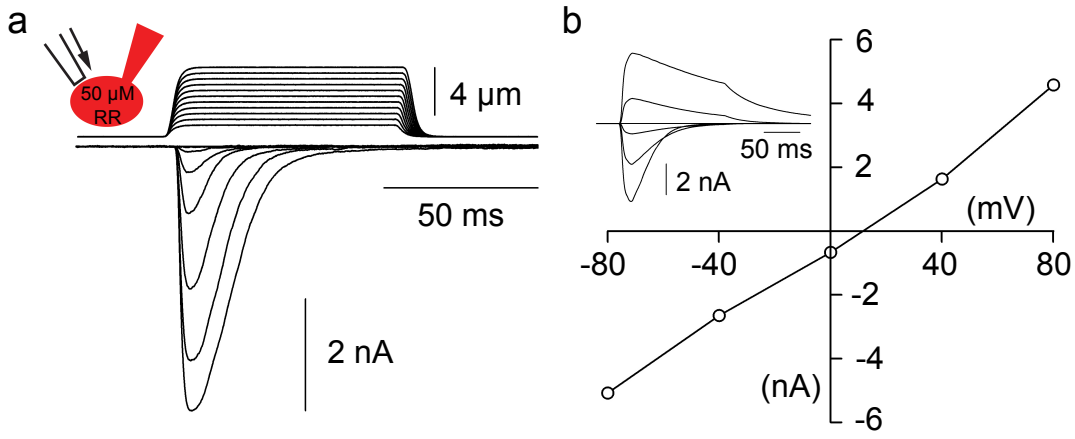

Supplementary Figure 2. Cytoplasmically applied RR does not affect mpiezo1 induced MA currents.

(a) Representative traces of whole cell MA inward currents in mpiezo1-transfected HEK293T cells at a holding potential of -80 mV. 50 µM RR is included in the recording electrode. (b) Current-voltage relationship of MA currents expressed in mpiezo1-transfected HEK293T cells when 50 µM RR is included in the recording electrode. (Inset) MA currents evoked at holding potentials ranging from -80 to +80 mV. Cells were perfused for at least 5 minutes prior to recordings.

Supplementary Figure 3

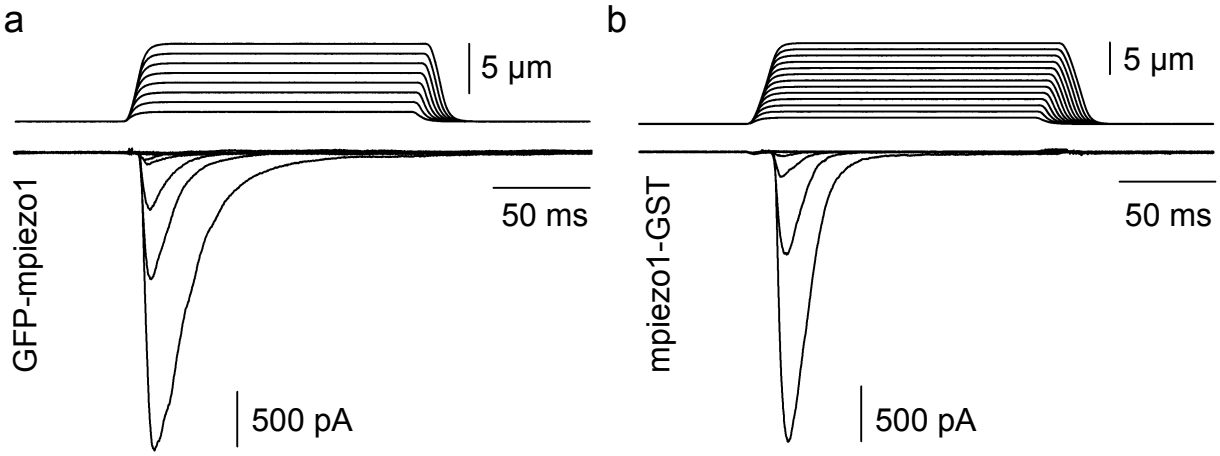

Supplementary Figure 3. GFP-mpiezo1 and mpiezo1-GST overexpression induce MA currents in HEK293T cells.

Representative traces of MA inward currents in GFP-mpiezo1- (a) and mpiezo1-GST- (b) transfected HEK293T cells recorded at a holding potential of -80 mV.

Supplementary Figure 4

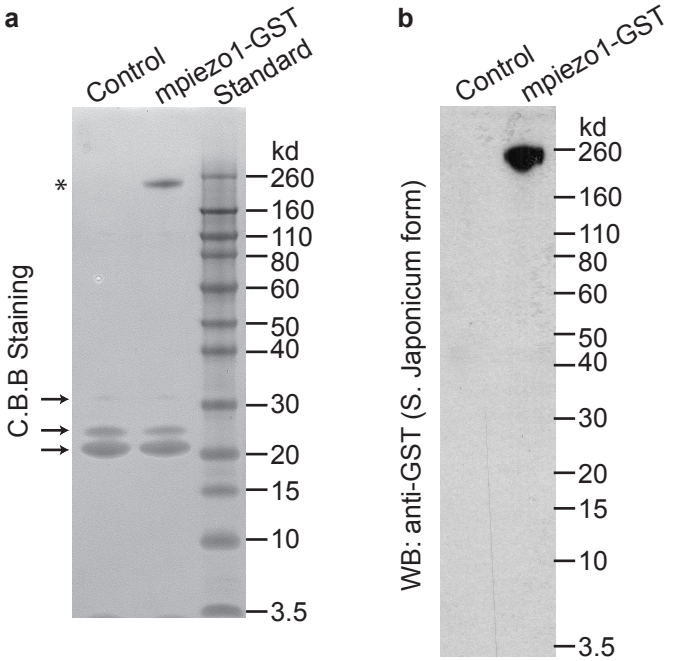

Supplementary Figure 4. Characterization of samples purified from HEK293T cells without transfection (control) or transfected with mpiezo1-GST (mpiezo1-GST) on denaturing gel.

Control and mpiezo1-GST samples were separated on a 4-12% Bis-Tris denaturing gel and visualized with Coomassie blue staining (a) or western blotting with an anti-GST (S. janonicum form) antibody (b). The Novex sharp pre-stained protein standards were used for indicating the molecular weights of proteins on the gel (a). A protein band at the position of the 260 kDa protein marker specifically present in the mpiezo1-GST sample correspond to mpiezo1-GST proteins, as confirmed by western blotting with the anti-GST antibody (Supplementary Fig. 4b) or an antibody specifically against piezo1 (Fig. 4). The three lower bands indicated by arrows correspond to endogenous glutathione S-transferase pi1 (GSTP1), glutathione S-transferase mu 3 (GSTM3), and carbonyl reductase 1 (CBR1), as identified by mass spectrometry of the gel slices containing the respective bands (data not shown) or the whole purified control and mpiezo1-GST samples (Supplementary Table 2). These proteins were pulled down by the glutathione beads. It should be noted that the anti-GST (S. janonicum form) antibody does not recognize the endogenous human GST isoforms.

Supplementary Figure 5

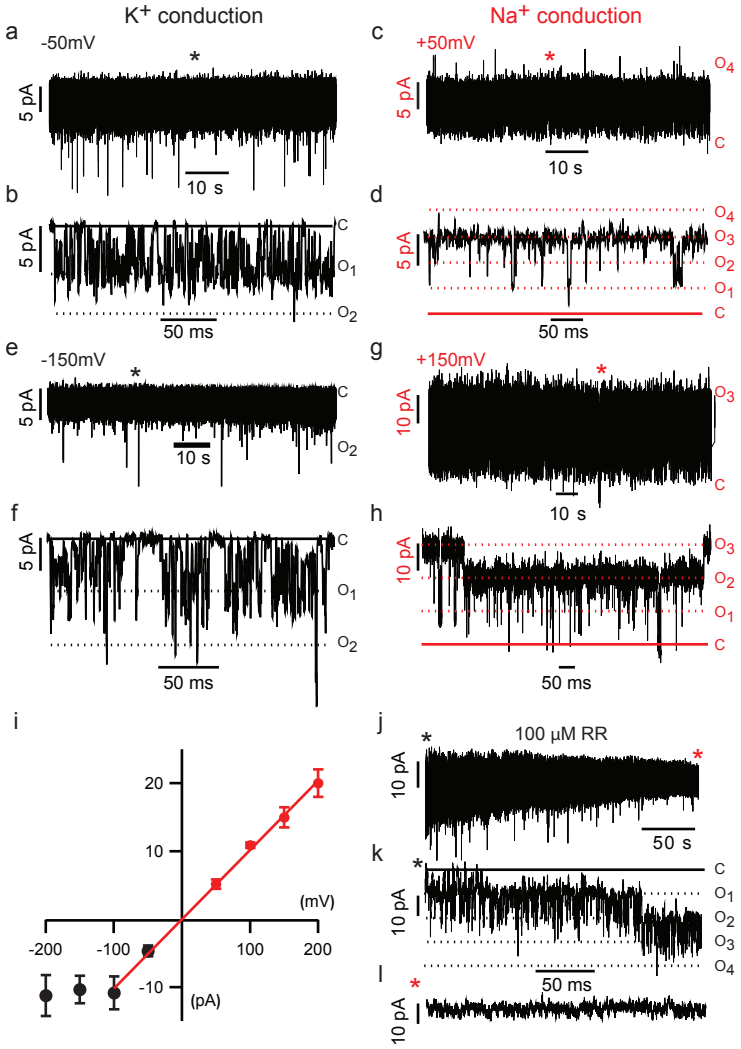

Supplementary Figure 5. mpiezo1 conduction under bi-ionic condition.

In the bi-ionic condition where the concentration of K^+ in the cytoplasm is 200 mM and the extracellular concentration of Na^+ is 200 mM, positive inward currents are carried by K^+ and negative outward currents are carried by Na^+. For comparison, ~2 min. recordings of inward (a, e) and outward (c, g) currents from a single experiment are shown at ±50 and ±150 mV. Segments indicated by an asterisk are displayed at higher time resolution (~ 250 to 500 ms) below the long recording to highlight few defined transitions between closed and open (b, f and d, h). At V=50 mV and V=–50 mV, the single channel inward K^+ current is 4.7 ± 0.8 pA (g=100±10 pS) (b) and the outward Na^+ current is 5.2 ±0.7 pA (g=90±10 pS) (d). The currents differ in that at –50 mV only 1 channel is carrying K^+ current while at +50 mV an average of 3 channels are passing Na^+. The inward permeation of K^+ appears transient assessed from the frequent short incomplete closures (b). This contrasts to the long uninterrupted outward Na^+ currents observed at –50 mV. When the potential difference is increased to 150 mV (±150 mV) the single channel inward K^+ current increases to only 10 ± 2 pA (g=70±10 pS)(b) whereas the outward Na^+ current increases to 15 ± 2 pA (g=100±10 pS)(d). At +150 mV, the Na^+ outward flux is stable as evidenced by long open times (g, h); at –150 mV, the transitions between open and closed states are faster than the time resolution of the recording and, accordingly, only a fraction of the single channel conductance is captured (e, f). This factor contributes significantly to the apparent saturation of K^+ inward current. A summary of the current–voltage relation for the channel under these bionic conditions extracted from 204,088 events distributed through three experiments is presented in panel i. A fit of the data with a linear function shows that the single channel current is ohmic between –100 and 200 mV with a slope conductance of 102 ± 2 pS. The current reversed direction at 0.0± 0.3 mV indicating that the channel does not select between K^+ and Na^+. To verify channel orientation, the experiment was terminated by the addition of RR (100 µM) to the bath (j, k, l). After an incubation time of 5 min at a resting potential of 0 mV, the membrane was hyperpolarized to –150 mV (j). A time expansion of the record at the pulse onset (k, black asterisk) shows that at least three channels were open and that these become progressively blocked. A time expansion of the record after ~4 minutes at –150 mV (l, red asterisk) indicates that the three channels are still active and that the single channel conductance has decreased to below measurable resolution.

Supplementary Figure 6

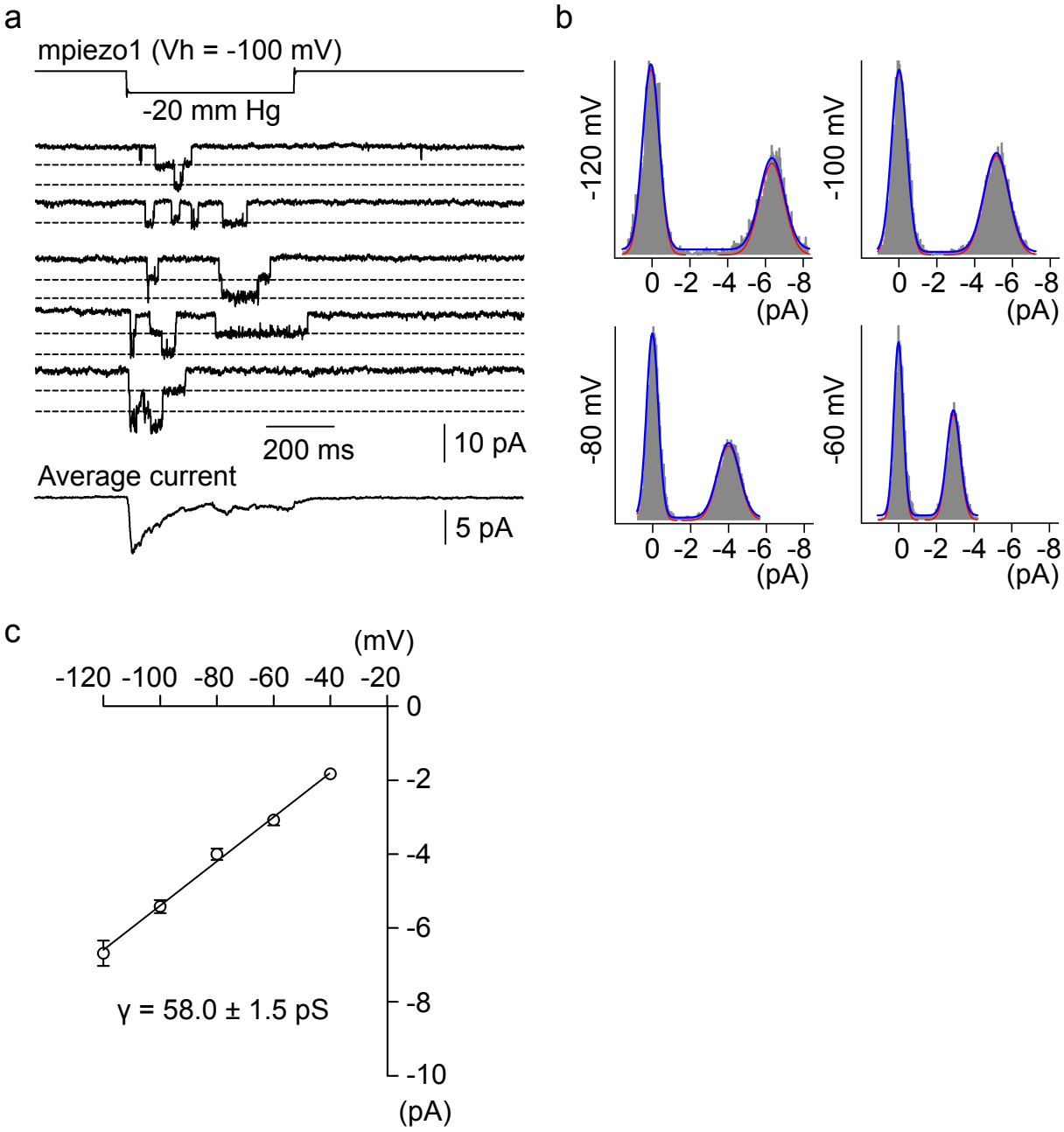

Supplementary Figure 6. Conductance characterization of mpiezo1-induced stretch-activated channels with divalent-free pipette solution.

(a) Representative stretch-activated channel openings elicited at -100 mV in mpiezo1-transfected cells in cell-attached configuration. The recording pipette was filled with a 150 mM NaCl solution. Bottom traces represent average of 40 individual recording traces. (b) All-point histograms of single channel opening events (average of 10 individual events) at holding potentials ranging from -120 to -60 mV. (c) Average current-voltage relationships of stretch activated single channels (n = 7 cells, respectively; mean ± s.e.m.). Single channel amplitude was determined as the amplitude difference in Gaussian fits as shown in b. The slope conductance value (γ) is the average of slope conductance values determined for each cell (mean ± s.e.m.).

Gel band containing control sample purified from either untransfected- (Exp1) or mock-transfected (Exp2) cells			
Protein hits	Gene information	Number of peptides identified in Exp 1	Number of peptides identified in Exp 2
gi|1346343 Keratin, type II cytoskeletal 1 (Cytokeratin-1) (CK-1) (Keratin-1) (K1) (67 kDa cytokeratin) (Hair alpha protein)	KRT1 gene	6	5
gi|28317 unnamed protein product [Homo sapiens]	Human gene for acidic (type I) cytokeratin 10	2	5
gi|119572363 hCG22067 [Homo sapiens]	From Homo sapiens 211000035830252 genomic scaffold, whole genome shotgun sequence	2	1
gi|494066 Chain A, Three-Dimensional Structure Of Class Pi Glutathione S- Transferase From Human Placenta In Complex With S- Hexylglutathione At 2.8 Angstroms Resolution	GSTP1 gene	2	0
gi|37460 unnamed protein product [Homo sapiens]	pancreatic trypsinogen III	1	1
gi|64653281 CHRNA4 protein [Homo sapiens]	CHRNA4	1	0
gi|5032087 splicing factor 3a, subunit 1, 120kDa isoform 1 [Homo sapiens]	splicing factor 3a, subunit 1, 120kDa	0	2
gi|55956899 keratin 9 [Homo sapiens]	KRT9 gene	0	1
gi|16751921 dermcidin preproprotein [Homo sapiens]	dermcidin	0	1
gi|547754 Keratin, type II cytoskeletal 2 epidermal (Cytokeratin-2e) (CK 2e) (K2e) (keratin-2)	KRT2 gene	0	1

Gel band containing samples purified from mpiezo1-GST transfected cells			
Protein hits	Gene information	Number of peptides identified in Exp 1	Number of peptides identified in Exp 2
mpiezo1-GST	**mPiezo1**	**32 (14% sequence coverage)**	**81 (31% sequence coverage)**
gi|1510143 KIAA0233 [Homo sapiens] (human piezo1)	**hPiezo1, likely detected from sequence homology with mPiezo1**	**7**	**12**
gi|307086 keratin-10	**KRT10 gene**	**2**	**0**
gi|386850 keratin K5	**KRT5 gene**	**0**	**3**
gi|119581150 keratin 14 (epidermolysis bullosa simplex, Dowling-Meara, Koebner), isoform CRA_b [Homo sapiens]	**KRT14 gene**	**0**	**2**
gi|6650826 PRO2044 [Homo sapiens]	**Serum albumin**	**1**	**0**
gi|6735452 B-ind1 protein [Homo sapiens]	**protein tyrosine phosphatase-like A domain containing 1**	**0**	**1**
gi|2224907 15S-lipoxygenase [Homo sapiens]	**arachidonate 15-lipoxygenase, type B**	**0**	**1**
gi|119595160 fibroblast growth factor 3 (murine mammary tumor virus integration site (v-int-2) oncogene homolog)	**fibroblast growth factor 3**	**0**	**1**
gi|1457948 APEG-1 protein	**SPEG complex locus**	**0**	**1**
gi|1346343 Keratin, type II cytoskeletal 1 (Cytokeratin-1) (CK-1) (Keratin-1) (K1) (67 kDa cytokeratin) (Hair alpha protein)	KRT1	6	14
gi|453155 keratin 9 [Homo sapiens]	KRT9 gene	4	11
gi|547754 Keratin, type II cytoskeletal 2 epidermal (Cytokeratin-2e) (CK 2e) (K2e) (keratin-2)	KRT2 gene	3	7
gi|494066 Chain A, Three-Dimensional Structure Of Class Pi Glutathione S- Transferase From Human Placenta In Complex With S- Hexylglutathione At 2.8 Angstroms Resolution	GSTP1	2	0
gi|119572363 hCG22067 [Homo sapiens]	From Homo sapiens 211000035830252 genomic scaffold, whole genome shotgun sequence	1	1
gi|28317 unnamed protein product [Homo sapiens]	Human gene for acidic (type I) cytokeratin 10	2	11
gi|37460 unnamed protein product [Homo sapiens]	pancreatic trypsinogen III	0	1

Supplementary Table 1. Mass spectrometry results of gel band containing samples purified from either control HEK293T cells (untransfected- or mock transfected-cells) or mpiezo1-GST transfected-cells.

Keratin proteins detected in both samples were likely derived from skin contamination during sample preparation. Among the proteins only detected in the mpiezo1-GST sample (highlighted in bold in the lower table), only piezo1 proteins were consistently identified with numerous peptides detected from two independent experiments.

Control sample purified from untransfected HEK293T cells			
Protein Hits	Gene Information	Number of Peptides Identified in Exp 1 (purified from whole cell lysate)	Number of Peptides Identified in Exp 2 (purified from membrane fraction)
gi|2554831 Chain A, Crystal Structure Of Human Glutathione S-Transferase P1- 1[v104] Complexed (9r,10r)-9-(S-Glutathionyl)-10- Hydroxy-9,10-Dihydrophenanthrene	glutathione S-transferase pi 1 (GSTP1)	12	7
gi|14250650 Glutathione S-transferase M3 (brain) [Homo sapiens]	glutathione S-transferase mu 3 (brain) (GSTM3)	6	
gi|157929330 glutathione S-transferase M2 (muscle) [Homo sapiens]	glutathione S-transferase mu 2 (muscle)	3	
gi|4502599 carbonyl reductase 1 [Homo sapiens]	carbonyl reductase 1 (CBR1)	1	1
gi|10835838 Chain L, Crystal Structure Of The Fab Fragment Of The Monoclonal Antibody Mak33		1	
gi|2345030 Ig kappa light chain variable region [Homo sapiens]		1	
gi|446244 anti-GlcNAc antibody variable region:SUBUNIT=heavy chain		1	
gi|49354807 immunoglobulin E variable region [Homo sapiens]		1	
gi|1346343 Keratin, type II cytoskeletal 1 (Cytokeratin-1) (CK-1) (Keratin-1)	Keratin 1		3
gi|453155 Keratin 9	Keratin 9		1
gi|5031931 nascent polypeptide-associated complex alpha subunit isoform b [Homo sapiens]	nascent polypeptide-associated complex alpha subunitprovided		1

mpiezo1-GST samples purified from mpiezo1-GST transfected HEK293T Cells			
Protein Hits	Gene Information	Number of Peptides Identified in Exp 1 (purified from whole cell lysate)	Number of Peptides Identified in Exp 2 (purified from membrane fraction)
mpiezo1-GST	**mpiezo1**	**4 (2% sequence coverage)**	**8 (4% sequence coverage)**
hCG1980844, isoform CRA_i [Homo sapiens]	**hpiezo1**		**1**
gi|2554831 Chain A, Crystal Structure Of Human Glutathione S-Transferase P1- 1[v104] Complexed (9r,10r)-9-(S-Glutathionyl)-10- Hydroxy-9,10-Dihydrophenanthrene	Glutathione S-transferase pi (GSTP1)	12	3
gi|14250650 Glutathione S-transferase M3 (brain) [Homo sapiens]	glutathione S-transferase mu 3 (brain) (GSTM3)	2	
gi|4502599 Carbonyl reductase 1 [Homo sapiens]	carbonyl reductase 1 (CBR1)	2	
gi|494186 Chain A, Crystal Structure Of Human Class Mu Glutathione Transferase Gstm2-2: Effects Of Lattice Packing On Conformational Heterogeneity	**glutathione S-transferase mu 2 (muscle) (GSTM2)**	**2**	

Supplementary Table 2. Mass spectrometry results of solution samples purified from either control untransfected HEK293T cells or mpiezo1-GST transfected cells.

Control and mpiezo1-GST samples purified from either whole cell lysates (Experiment 1) or membrane fractions (Experiment 2). GSTP1, GSTM3, CBR1 proteins were consistently identified in both control and mpiezo1-GST samples, corresponding to the three lower protein bands present in both control and mpiezo1-GST sample (Supplementary Fig. 4a). mpiezo1-GST proteins were consistently identified only in the mpiezo1-GST sample. Reconstitution of the same set of samples used for experiment 2 into lipid bilayers resulted in recordings of channel activity with mpiezo1-GST but not control sample, suggesting that the observed channel activity is specifically mediated by mpiezo1-GST proteins.

Conductance (pS)	118 ± 15
Open Occupancy	0.43 ± 0.14
Closed occupancy	0.57 ± 0.15
τ_{open} **(ms)**	13 ± 4
$\tau_{1closed}$ **(ms)**	5 ± 1 (0.74)
$\tau_{2closed}$ **(ms)**	47 ± 9 (0.26)
Total number of openings	19,583

Supplementary Table 3. Single channel properties of mpiezo1 in lipid bilayers.

Single channel current recordings, in which only one channel was open at any given time, were analyzed to determine the channel dwell times in the open and closed states (references 1 and 2). Probability density analysis provides the number of open and closed states and the channel open (τ_o) and closed (τ_c) lifetimes (refs 1 and 2). Histograms were normalized to have a total area equal to one. The data summarized in the Table provide evidence for the occurrence of a single open state and two closed states under the experimental conditions (0.5 M KCl and V=–100 mV). For τ_{c1} and τ_{c2} , the relative area under the fitted curve is shown in brackets and represents the frequency of occurrence of each state. The results are cumulative from three different experiments; error indicates s.e.m.

1. Labarca, P., J.A. Rice, D.R. Fredkin and M. Montal. 1985. Kinetic analysis of channel gating: Application to the cholinergic receptor channel and the chloride channel from *Torpedo californica*. *Biophys. J.* 47:469-478.

2. Keller BU, Hartshorne RP, Talvenheimo JA, Catterall WA, Montal M. 1986.Sodium channels in planar lipid bilayers. Channel gating kinetics of purified sodium channels modified by batrachotoxin. *J Gen Physiol* 88: 1-23.